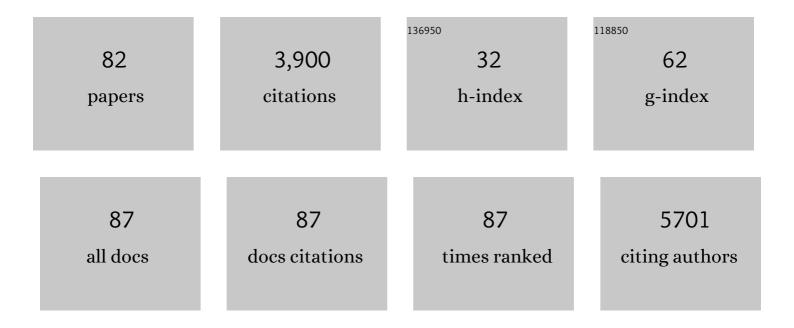
Chun-Hu Chen

List of Publications by Year in descending order

Source: https://exaly.com/author-pdf/4077376/publications.pdf Version: 2024-02-01



#	Article	IF	CITATIONS
1	Highly-Oxidized Graphene Oxide for Achieving Low-Loss Hybrid Waveguide Gratings on SOI. IEEE Journal of Selected Topics in Quantum Electronics, 2022, 28, 1-9.	2.9	2
2	Enhanced Thermal Conducting Behavior of Pressurized Graphene-Silver Flake Composites. Langmuir, 2022, 38, 727-734.	3.5	6
3	Rubâ€Resistant Antibacterial Surface Conversion Layer on Stainless Steel. Advanced Materials Interfaces, 2022, 9, .	3.7	7

Rubâ \in Resistant Antibacterial Surface Conversion Layer on Stainless Steel (Adv. Mater. Interfaces) Tj ETQq0 0 0 rgB $\frac{1}{3}$. Overlock 10 Tf 50 overlock

5	Laser-Accelerated Mass Transport in Oxygen Reduction Via a Graphene-Supported Silver–Iron Oxide Heterojunction. Journal of Physical Chemistry Letters, 2022, 13, 4200-4206.	4.6	2
6	Activation Energy Assessing Potential-Dependent Activities and Site Reconstruction for Oxygen Evolution. ACS Energy Letters, 2022, 7, 2236-2243.	17.4	14
7	Rational design of hetero-dimensional C-ZnO/MoS2 nanocomposite anchored on 3D mesoporous carbon framework towards synergistically enhanced stability and efficient visible-light-driven photocatalytic activity. Chemosphere, 2021, 266, 129148.	8.2	28
8	Magnetic hollow buoyant alginate beads achieving rapid remediation of oil contamination on water. Journal of Environmental Chemical Engineering, 2021, 9, 104935.	6.7	7
9	Efficient One-Step Conversion of a Low-Grade Vegetable Oil to Biodiesel over a Zinc Carboxylate Metal–Organic Framework. ACS Omega, 2021, 6, 1834-1845.	3.5	18
10	Rock Salt Oxide Hollow Spheres Achieving Durable Performance in Bifunctional Oxygen Energy Cells. ACS Applied Energy Materials, 2021, 4, 3448-3459.	5.1	10
11	Microâ€droplet Trapping and Manipulation: Understanding Aerosol Better for a Healthier Environment. Chemistry - an Asian Journal, 2021, 16, 1644-1660.	3.3	3
12	Cobalt Iron Oxides Prepared by Acidic Redox-Assisted Precipitation: Characterization, Applications, and New Opportunities. ACS Applied Materials & Interfaces, 2021, , .	8.0	2
13	Role of carrier-transfer in the optical nonlinearity of graphene/Bi ₂ Te ₃ heterojunctions. Nanoscale, 2020, 12, 16956-16966.	5.6	20
14	Gold Nanoparticles Grown by Galvanic Replacement on Graphene-Coated Aluminum Panels as Large-Area Substrates for Surface-Enhanced Raman Scattering. ACS Applied Nano Materials, 2020, 3, 5783-5793.	5.0	9
15	Facile Bottom-up Preparation of WS2-Based Water-Soluble Quantum Dots as Luminescent Probes for Hydrogen Peroxide and Glucose. Nanoscale Research Letters, 2019, 14, 271.	5.7	28
16	Regenerable Acidity of Graphene Oxide in Promoting Multicomponent Organic Synthesis. Scientific Reports, 2019, 9, 15579.	3.3	28
17	Discontinuityâ€Enhanced Thin Film Electrocatalytic Oxygen Evolution. Small, 2019, 15, e1903363.	10.0	11
18	Molecular Approach To Enhance Thermal Conductivity in Electrically Conductive Adhesives. ACS Applied Electronic Materials, 2019, 1, 1890-1898.	4.3	10

#	Article	IF	CITATIONS
19	Binder-free graphene oxide doughs. Nature Communications, 2019, 10, 422.	12.8	44
20	Removal of chlorpheniramine and variations of nitrosamine formation potentials in municipal wastewaters by adsorption onto the GO-Fe3O4. Environmental Science and Pollution Research, 2019, 26, 20701-20711.	5.3	12
21	Two-photon absorption within layered Bi ₂ Te ₃ topological insulators and the role of nonlinear transmittance therein. Journal of Materials Chemistry C, 2019, 7, 7027-7034.	5.5	26
22	Electrocatalytic Oxygen Evolution: Discontinuityâ€Enhanced Thin Film Electrocatalytic Oxygen Evolution (Small 50/2019). Small, 2019, 15, 1970270.	10.0	0
23	Binary Cobalt Manganese Oxide Systems for Electrocatalytic Applications. ECS Meeting Abstracts, 2019, , .	0.0	0
24	Facile and Costâ€Efficient Synthesis of Quasiâ€0D/2D ZnO/MoS ₂ Nanocomposites for Highly Enhanced Visibleâ€Lightâ€Driven Photocatalytic Degradation of Organic Pollutants and Antibiotics. Chemistry - A European Journal, 2018, 24, 9305-9315.	3.3	61
25	Facet-specific heterojunction in gold-decorated pyramidal silicon for electrochemical hydrogen peroxide sensing. Sensors and Actuators B: Chemical, 2018, 266, 463-471.	7.8	19
26	Achieving Solidification and Redispersion of Semiconducting Polymer Dots by Layered Double Hydroxide Incorporation. ACS Applied Nano Materials, 2018, 1, 55-64.	5.0	7
27	Si photonics waveguide Bragg reflector based on thin graphene oxide grating overlay. , 2018, , .		0
28	Heterojunctions of silver–iron oxide on graphene for laser-coupled oxygen reduction reactions. Chemical Communications, 2018, 54, 7900-7903.	4.1	23
29	Redox-assisted multicomponent deposition of ultrathin amorphous metal oxides on arbitrary substrates: highly durable cobalt manganese oxyhydroxide for efficient oxygen evolution. Journal of Materials Chemistry A, 2018, 6, 17915-17928.	10.3	20
30	Light-Emitting Illumination and Field Emission Device of Potassium Hydroxide-Doped Electrochemically Reduced Graphene Oxide. IEEE Transactions on Electron Devices, 2017, 64, 2251-2256.	3.0	2
31	Effective Synthesis of Highly Oxidized Graphene Oxide That Enables Wafer-scale Nanopatterning: Preformed Acidic Oxidizing Medium Approach. Scientific Reports, 2017, 7, 3908.	3.3	43
32	The Effect of Surface Pretreatment on the Corrosion Performance of Graphene Coatings on 6061 Aluminum Alloy. ECS Transactions, 2017, 77, 693-703.	0.5	2
33	Different influences of nanopore dimension and pH between chlorpheniramine adsorptions on graphene oxide-iron oxide suspension and particle. Chemical Engineering Journal, 2017, 307, 447-455.	12.7	27
34	Narrowband silicon waveguide Bragg reflector achieved by highly ordered graphene oxide gratings. Optics Letters, 2017, 42, 4768.	3.3	11
35	Weakly-coupled Si waveguide Bragg reflector enabled by precisely-controlled graphene oxide gratings. , 2017, , .		0

36 Silicon/Graphene Oxide Hybrid Photonic Waveguide Filter. , 2016, , .

0

#	Article	IF	CITATIONS
37	Enhanced Photocatalytic Performance of ZnO Nanorods Coupled by Twoâ€Dimensional αâ€MoO ₃ Nanoflakes under UV and Visible Light Irradiation. Chemistry - A European Journal, 2016, 22, 12777-12784.	3.3	27
38	Full Solutionâ€Processed Synthesis and Mechanisms of a Recyclable and Bifunctional Au/ZnO Plasmonic Platform for Enhanced UV/Vis Photocatalysis and Optical Properties. Chemistry - A European Journal, 2016, 22, 14950-14961.	3.3	29
39	General Solvent-dependent Strategy toward Enhanced Oxygen Reduction Reaction in Graphene/Metal Oxide Nanohybrids: Effects of Nitrogen-containing Solvent. Scientific Reports, 2016, 6, 37174.	3.3	21
40	Mechanistic insights into light-driven graphene-induced peroxide decomposition: radical generation and disproportionation. Chemical Communications, 2016, 52, 9291-9294.	4.1	5
41	Photochemical Green Synthesis of Nanostructured Cobalt Oxides as Hydrogen Peroxide Redox for Bifunctional Sensing Application. Electrochimica Acta, 2016, 190, 588-595.	5.2	23
42	Thin and Transferrable Graphene Oxide Grating Layer. , 2016, , .		0
43	Field emission of electrochemical graphene oxide. , 2015, , .		1
44	Hybridization of Graphene in 3D Complex Nanovoids: Synergistic Nanocomposites for Electrocatalytic Reduction of Hydrogen Peroxide. Electrochimica Acta, 2015, 180, 1014-1022.	5.2	16
45	Structural Distortion of Molybdenum-Doped Manganese Oxide Octahedral Molecular Sieves for Enhanced Catalytic Performance. Inorganic Chemistry, 2015, 54, 10163-10171.	4.0	78
46	Graphene thickness-controlled photocatalysis and surface enhanced Raman scattering. Nanoscale, 2014, 6, 12805-12813.	5.6	41
47	Redox preparation of mixed-valence cobalt manganese oxide nanostructured materials: highly efficient noble metal-free electrocatalysts for sensing hydrogen peroxide. Nanoscale, 2014, 6, 334-341.	5.6	98
48	Hierarchical nanostructures with unique Y-shaped interconnection networks in manganese substituted cobalt oxides: the enhancement effect on electrochemical sensing performance. Chemical Communications, 2013, 49, 3025.	4.1	23
49	Site-specific stamping of graphene micro-patterns over large areas using flexible stamps. Nanotechnology, 2012, 23, 235603.	2.6	5
50	Control of Catalytic Activity Via Porosity, Chemical Composition, and Morphology of Nanostructured Porous Manganese Oxide Materials. Journal of the Chinese Chemical Society, 2012, 59, 465-472.	1.4	15
51	Plasma sprayed gadolinium zirconate thermal barrier coatings that are resistant to damage by molten Ca–Mg–Al–silicate glass. Surface and Coatings Technology, 2012, 206, 3911-3916.	4.8	110
52	A Foaming Esterification Sol–Gel Route for the Synthesis of Magnesia–Yttria Nanocomposites. Journal of the American Ceramic Society, 2011, 94, 367-371.	3.8	29
53	Manganese Oxide Octahedral Molecular Sieves (OMS-2) Multiple Framework Substitutions: A New Route to OMS-2 Particle Size and Morphology Control. Advanced Functional Materials, 2011, 21, 312-323.	14.9	157
54	Preferential oxidation of CO in H2-rich feeds over mesoporous copper manganese oxides synthesized by a redox method. International Journal of Hydrogen Energy, 2011, 36, 6768-6779.	7.1	49

#	Article	IF	CITATIONS
55	ZnO/La2O2CO3 layered composite: A new heterogeneous catalyst for the efficient ultra-fast microwave biofuel production. Applied Catalysis B: Environmental, 2011, 103, 200-205.	20.2	47
56	High quality, transferrable graphene grown on single crystal Cu(111) thin films on basal-plane sapphire. Applied Physics Letters, 2011, 98, .	3.3	113
57	Titanium Containing γâ€MnO ₂ (TM) Hollow Spheres: Oneâ€Step Synthesis and Catalytic Activities in Li/Air Batteries and Oxidative Chemical Reactions. Advanced Functional Materials, 2010, 20, 3373-3382.	14.9	146
58	Nanoscale manganese oxide octahedral molecular sieves (OMS-2) as efficient photocatalysts in 2-propanol oxidation. Applied Catalysis A: General, 2010, 375, 295-302.	4.3	85
59	Total oxidation of CO at ambient temperature using copper manganese oxide catalysts prepared by a redox method. Applied Catalysis B: Environmental, 2010, 99, 103-110.	20.2	159
60	Heteroepitaxial Growth of Nanoscale Oxide Shell/Fiber Superstructures by Mild Hydrothermal Processes. Small, 2010, 6, 988-992.	10.0	16
61	Nanostructured arrays of semiconducting octahedral molecular sieves by pulsed-laser deposition. Nature Materials, 2010, 9, 54-59.	27.5	29
62	Hydrophobic Polymer-Coated Metal Oxide Catalysts for Effective Low-Temperature Oxidation of CO under Moisture-Rich Conditions. Chemistry of Materials, 2010, 22, 3313-3315.	6.7	34
63	Microwave-Assisted Hydrothermal Synthesis of Cryptomelane-Type Octahedral Molecular Sieves (OMS-2) and Their Catalytic Studies. Chemistry of Materials, 2010, 22, 3664-3669.	6.7	89
64	Single-step synthesis of manganese oxide octahedral molecular sieves with large pore sizes. Chemical Communications, 2010, 46, 5945.	4.1	31
65	Microwave-Assisted Synthesis of Manganese Oxide Octahedral Molecular Sieve (OMS-2) Nanomaterials under Continuous Flow Conditions. Journal of Physical Chemistry C, 2010, 114, 14417-14426.	3.1	51
66	Removal of Aqueous Phenol by Adsorption and Oxidation with Doped Hydrophobic Cryptomelane-Type Manganese Oxide (Kâ^'OMS-2) Nanofibers. Journal of Physical Chemistry C, 2010, 114, 9835-9844.	3.1	68
67	Manganese octahedral molecular sieve catalysts for selective styrene oxide ring opening. Catalysis Today, 2009, 140, 162-168.	4.4	30
68	γ-MnO2 octahedral molecular sieve: Preparation, characterization, and catalytic activity in the atmospheric oxidation of toluene. Applied Catalysis A: General, 2009, 355, 169-175.	4.3	34
69	ZnO with Different Morphologies Synthesized by Solvothermal Methods for Enhanced Photocatalytic Activity. Chemistry of Materials, 2009, 21, 2875-2885.	6.7	444
70	Green Decomposition of Organic Dyes Using Octahedral Molecular Sieve Manganese Oxide Catalysts. Journal of Physical Chemistry A, 2009, 113, 1523-1530.	2.5	92
71	Novel Urchin-like CuO Synthesized by a Facile Reflux Method with Efficient Olefin Epoxidation Catalytic Performance. Chemistry of Materials, 2009, 21, 1253-1259.	6.7	151
72	Controlled Synthesis of Selfâ€Assembled Metal Oxide Hollow Spheres Via Tuning Redox Potentials: Versatile Nanostructured Cobalt Oxides. Advanced Materials, 2008, 20, 1205-1209.	21.0	92

#	Article	IF	CITATIONS
73	Framework Doping of Indium in Manganese Oxide Materials: Synthesis, Characterization, and Electrocatalytic Reduction of Oxygen. Chemistry of Materials, 2008, 20, 2069-2071.	6.7	56
74	3D Flowerlike α-Nickel Hydroxide with Enhanced Electrochemical Activity Synthesized by Microwave-Assisted Hydrothermal Method. Chemistry of Materials, 2008, 20, 308-316.	6.7	419
75	Systematic Control of Particle Size in Rapid Open-Vessel Microwave Synthesis of K-OMS-2 Nanofibers. Journal of Physical Chemistry C, 2008, 112, 6786-6793.	3.1	64
76	Effect of Microwave Frequency on Hydrothermal Synthesis of Nanocrystalline Tetragonal Barium Titanate. Journal of Physical Chemistry C, 2008, 112, 9659-9667.	3.1	97
77	Ultrasonic Nozzle Spray in Situ Mixing and Microwave-Assisted Preparation of Nanocrystalline Spinel Metal Oxides:  Nickel Ferrite and Zinc Aluminate. Journal of Physical Chemistry C, 2008, 112, 1407-1414.	3.1	67
78	A Designed Single-Step Method for Synthesis and Structural Study of Organicâ^'Inorganic Hybrid Materials: Well-Ordered Layered Manganese Oxide Nanocomposites. Journal of the American Chemical Society, 2008, 130, 14390-14391.	13.7	33
79	Syntheses of Nanostructures of Cobalt Hydrotalcite Like Compounds and Co ₃ O ₄ via a Microwave-Assisted Reflux Method. Journal of Physical Chemistry C, 2008, 112, 8177-8183.	3.1	85
80	New Synthetic Route, Characterization, and Electrocatalytic Activity of Nanosized Manganite. Chemistry of Materials, 2007, 19, 1832-1839.	6.7	90
81	Catalytic synthesis, characterization and magnetic properties of iron phosphide nanowires. Journal of Materials Chemistry, 2004, 14, 296-298.	6.7	44
82	Evolution of optical nonlinearity within graphene/Bi ₂ Te ₃ heterostructure. Journal of Materials Chemistry C, 0, , .	5.5	3